https://doi.org/10.5194/bg-2022-119
Preprint. Discussion started: 19 May 2022

Biogeosciences Discussions

Title: Drifting macrophyte detritus triggers 'hidden' benthic hypoxia

Author list: Karl M. Attard[1,2,3], Anna Lyssenko[3], Iván F. Rodil[3,4]

Corresponding author: Karl M. Attard karl.attard@biology.sdu.dk

Author affiliations:

[1] Department of Biology, University of Southern Denmark, 5230 Odense M, Denmark

[2] Danish Institute for Advanced Study, University of Southern Denmark, 5230 Odense M, Denmark

[3] Tvärminne Zoological Station, University of Helsinki, J.A. Palménin tie 260, 10900 Hanko, Finland

[4] Department of Biology (INMAR), Faculty of Marine and Environmental Sciences, University of Cádiz, Puerto Real, Spain

Keywords: benthic ecosystems, primary production, respiration, oxygen fluxes, biodiversity

Abstract

Macrophytes form highly productive habitats that export a substantial proportion of their primary production as particulate organic matter. As the detritus drifts with currents and accumulates in seafloor depressions, it constitutes organic enrichment and can deteriorate O_2 conditions on the seafloor. In this study, we investigate the O_2 dynamics and macrobenthic biodiversity associated with a shallow ~2300 m^2 macrophyte detritus field in the northern Baltic Sea. The detritus, primarily *Fucus vesiculosus* fragments, had a biomass of ~1700 g dry weight m^{-2}, approximately 1.5-fold larger than nearby intact *F. vesiculosus* canopies. A vertical array of O_2 sensors placed within the detritus documented that hypoxia ($[O_2] < 63$ µmol L^{-1}) occurred for 23% of the time and terminated at the onset of wave-driven hydrodynamic mixing. Measurements in five other habitats nearby spanning bare sediments, seagrass, and macroalgae indicate that hypoxic conditions were unique to detritus canopies. Fast-response O_2 sensors placed above the detritus documented pulses of hypoxic waters originating from within the canopy. These pulses triggered a rapid short-term (~5 min) deterioration of O_2 conditions within the water column. Eddy covariance measurements of O_2 fluxes indicated that daily photosynthetic production offset up to 81 % of the respiratory demands of the detritus canopy, prolonging its persistence within the coastal zone. The detritus site had a low

https://doi.org/10.5194/bg-2022-119
Preprint. Discussion started: 19 May 2022

abundance of crustaceans, bivalves, and polychaetes when compared to other habitats nearby, likely because their low-O_2 tolerance thresholds were often exceeded.

1. Introduction

Oxygen availability determines ecosystem health and the biogeochemical function of coastal waters (Diaz and Rosenberg, 2008; Middelburg and Levin, 2009; Breitburg et al., 2018). When in gaseous equilibrium with air, seawater typically contains an O_2 concentration ($[O_2]$) between 200-400 µmol L^{-1}, depending on the water temperature and the salinity (Garcia and Gordon, 1992). However, both abiotic and biotic processes cause significant departures from equilibrium. The main source of O_2 to coastal waters is the atmosphere, where the diffusion of O_2 is governed by the air-to-sea gas exchange rate (Berg and Pace, 2017; Long and Nicholson, 2018). In shallow waters and light-exposed seafloor sediments, O_2 is produced by primary producers as a by-product of photosynthesis, and it is consumed by consortia of microbes and fauna directly, through aerobic respiration, and indirectly, through the oxidation of reduced substances (Glud, 2008). If O_2 consumption exceeds supply for a sufficiently long period, O_2 conditions deteriorate and become hypoxic ($[O_2] < 63$ µmol L^{-1}). Hypoxia is becoming more common, more intense, and is affecting larger areas of coastal waters, increasingly placing ecosystems and the services they provide at risk (Breitburg et al., 2018). There are several well-known variants of coastal hypoxia (Diaz and Rosenberg, 2008). Seasonal hypoxia, the most common form, typically occurs in summer when warm waters, strong stratification, and high organic enrichment combine to deplete O_2 until autumn (Robertson et al., 2016). Periodic O_2 depletion, in contrast, occurs more often due to local weather dynamics and tidal cycles but individual events are shorter (Diaz and Rosenberg, 1995), whereas diel cycles with large day-to-night $[O_2]$ excursions trigger hypoxia for a few hours daily (Davanzo and Kremer, 1994; Tyler et al., 2009). All events are expected to affect biodiversity and biogeochemical cycling to varying degrees. Seasonal hypoxia and periodic O_2 depletion are associated with large-scale mortality of organisms and a switch between retention and removal of bioavailable nutrients such as nitrate, ammonium, phosphate, and toxic hydrogen sulfide (Middelburg and Levin, 2009). Short-term hypoxic events can similarly exceed lethal and non-lethal thresholds for many benthic taxa (Vaquer-Sunyer and Duarte, 2008), although, due to their sporadic nature, their occurrence and impacts are less understood.

Given the importance of O_2 in coastal waters, $[O_2]$ is one of the most frequently measured environmental parameters. Near-seabed O_2 availability is typically measured using long-term stable

https://doi.org/10.5194/bg-2022-119
Preprint. Discussion started: 19 May 2022

O_2 sensors (e.g. optodes, Bittig et al. (2018)) that are moored ~0.5 m above the seafloor, or by performing vertical profiles of water column [O_2] down to ~1.0 m above the seafloor using multiparameter sondes. National monitoring programs such as those maintained by the Swedish Meteorological and Hydrological Institute and the Finnish Environment Institute provide a wealth of essential open-access data, enabling important analyses detailing the prevalence and intensity of coastal hypoxia (Virtanen et al., 2019). Notwithstanding the progress being made in coastal monitoring, it was demonstrated more than 40 years ago that the largest [O_2] gradients may occur just a few cm above the seafloor due to the high reactivity of marine sediments and a strong benthic O_2 demand (Jorgensen, 1980). Hypoxic conditions affecting the seafloor may therefore remain 'hidden' if sensors are located higher up in the water column, as is common practice.

Around two-thirds of the ocean's photosynthetic biomass is bound in macrophytes growing in shallow waters along the world's coastline (Smith, 1981). Through seasonal decay, epiphyte growth, grazing, and physical forcing (e.g. waves, currents, ice scouring), macrophytes export a large proportion of their primary production (~40 %) to their surroundings as detritus (Attard et al., 2019a; Krumhansl and Scheibling, 2012; Duarte and Cebrián, 1996). Macrophyte detritus drifts with the currents and accumulates on the shoreline and in low-energy marine environments (e.g. shallow seafloor depressions and in deeper waters), where it constitutes habitat structure and organic enrichment to the receiving habitat (Norkko and Bonsdorff, 1996b). Given high enough abundance, detritus suppresses the diffusion of O_2 from the water column to the sediment surface and it exacerbates O_2 depletion on the seabed as it decays. Large accumulations of unattached ephemeral macroalgae such as the brown algae *Ectocarpus siliculosus* and *Pylaiella littoralis* are common in eutrophic coastal waters such as the Baltic Sea, forming thin mats above the seafloor typically a few centimeters thick (Norkko and Bonsdorff, 1996a). Large accumulations of detritus produced from perennial brown seaweeds have also been observed (Glud et al., 2004). However, the O_2 dynamics within accumulations of drifting detritus and the potential implications for the associated fauna remain poorly understood. Understanding the ecological and biogeochemical implications of drifting macrophyte detritus is particularly important given the ambitions to vastly increase macroalgal farming, which would result in increased deposition of macrophyte detritus on the coastal seafloor (Broch et al., 2019; Broch et al., 2022).

In this study, we investigate the O_2 dynamics and macrobenthic biodiversity associated with a shallow ~2300 m^2 macrophyte detritus field composed of *Fucus vesiculosus* fragments in the northern Baltic Sea. To assess O_2 production versus consumption rates of the detritus canopy, we

https://doi.org/10.5194/bg-2022-119
Preprint. Discussion started: 19 May 2022

deployed an eddy covariance system on multiple occasions to extract benthic O_2 fluxes non-invasively. Using a vertical array of O_2 sensors and an acoustic velocimeter, we monitored O_2 distribution within the canopy and the hydrodynamics above the canopy to assess the occurrence and intensity of hypoxic events and their links to local hydrodynamics. We performed biodiversity surveys to identify the prevailing taxa, and we compared hypoxic thresholds of these taxa to [O_2] measured *in situ* to identify potential stress. Measurements were also performed in five other habitats nearby spanning bare sediments, seagrass, and macroalgae for comparison.

2. Materials and Methods

2.1. Study location

The study was performed in the microtidal Baltic Sea nearby the Tvärminne Zoological Station in SW Finland. Although the focus of our study was to investigate drifting macrophyte detritus, we selected an additional five study sites within the shallow subtidal zone (2-4 m depth) for comparison, representing key habitats in the Baltic Sea: one site with bare sediments, two sites with seagrass (predominantly *Zostera marina*; sheltered and exposed), and two sites with intact macroalgae canopies (predominantly *Fucus vesiculosus*; sheltered and exposed) (Table 1).

Table 1: Environmental conditions and low-oxygen events at the six study sites

Site	Location	Deployment start	Deployment duration (h)	Water depth (m)	Water temperature (°C)	Minimum O_2 (µmol L^{-1})	Maximum O_2 (µmol L^{-1})	Hypoxia duration (h)
Macrophyte detritus	59 811613 N 23 206624 E	29-05-2018	120	3.0	12	0.6	429	27
Bare sediments	59 841532 N 23 253370 E	20-05-2018	96	3.7	11	307	407	0
Sheltered *Z. marina*	59 841551 N 23 251203 E	27-05-2018	87	4.0	16	272	333	0
Exposed *Z. marina*	59 827008 N 23 151976 E	08-06-2018	120	2.9	10	281	437	0
Sheltered *F. vesiculosus*	59 826856 N 23 209721 E	08-06-2018	120	2.0	10	253	489	0
Exposed *F. vesiculosus*	59 811359 N 23 207281 E	01-06-2018	116	2.0	9	287	427	0

2.2. O_2 dynamics of benthic habitats

To investigate the near-bed O_2 dynamics and its environmental controls, we equipped a tripod frame with a suite of sensors consisting of three cross-calibrated dissolved O_2 loggers with inbuilt temperature compensation (HOBO U26-001, Onset), a 6 MHz acoustic velocimeter (Vector, Nortek), a photosynthetic active radiation (PAR) sensor (RBRsolo with Licor PAR Quantum

https://doi.org/10.5194/bg-2022-119
Preprint. Discussion started: 19 May 2022

192SA), and a saltwater conductivity sensor (HOBO U24-002-C). The O_2 loggers have a factory-specified accuracy of ± 6 µmol L^{-1} from 0 to 250 µmol L^{-1}, ± 16 µmol L^{-1} from 250-625 µmol L^{-1}, a resolution of 0.6 µmol L^{-1} and a 90% response time (T_{90}) < 2 min. The O_2 and conductivity sensors were mounted onto a 75 cm-long stainless steel rail affixed to the tripod leg (Fig. 1). The sensors were secured to the rail at various heights above the seabed using rail mount clamps. For the study sites with canopies, two sensors were set inside the canopy; one sensor was ~5 cm above the seafloor and one was close to the top of the canopy (15-25 cm). The third sensor was placed in the water above the canopy (~35 cm above the seafloor). The tripod was deployed by divers from a small boat and was carefully positioned on the seafloor using a lift bag. The exact sensor heights were noted by the divers once the instrument was on the seafloor. The instrument was left to record data for 3-5 days at each site. The velocimeter sampled three-dimensional flow velocity continuously at 8 Hz, whereas the O_2, temperature, conductivity, and PAR sensors recorded data every minute.

To investigate O_2 dynamics and its environmental drivers, all sensor time series were aligned in time and analyses were performed to investigate vertical gradients in O_2 distribution, diel O_2 excursions, and boundary-layer hydrodynamics. We assessed the occurrence of hypoxia (O_2 < 63 µmol L^{-1}) by quantifying the magnitude (lowest O_2 value) and the duration (in hours) of hypoxic events. The high-frequency velocity data were used to calculate mean flow velocity magnitude ($\overline{U}$) as the sum of streamwise (u) and traverse (v) components, as $\overline{U} = \sqrt{u^2 + v^2}$.

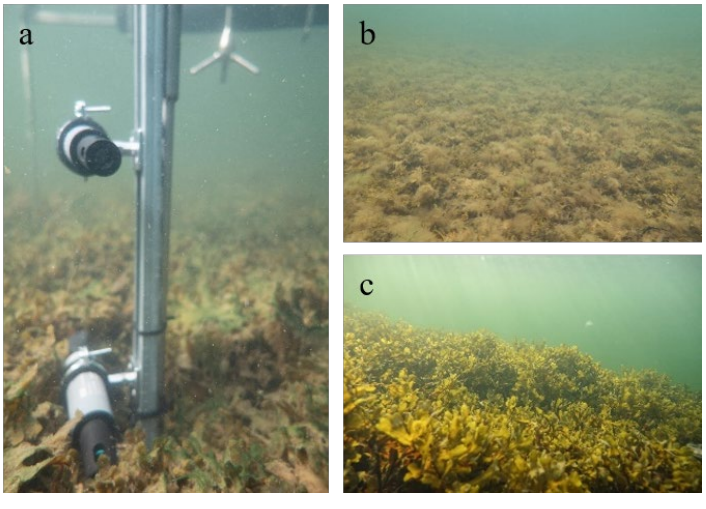

https://doi.org/10.5194/bg-2022-119
Preprint. Discussion started: 19 May 2022

Fig. 1: The study area showing (a) the instrument deployed within the detritus canopy, (b) a broad-scale view of the detritus accumulation area, and (c) a nearby *Fucus vesiculosus* canopy.

2.3. Benthic O_2 fluxes

An aquatic eddy covariance system was deployed at the detritus site to quantify benthic O_2 fluxes at the canopy-water interface on three occasions (June 2017, September 2017, and May 2018). The eddy covariance setup was identical to the tripod frame described above, with the addition of a fast-response (T_{90} < 0.3 s) O_2 microsensor setup for covariance measurements (Mcginnis et al., 2011). The hardware and data processing techniques are described in detail in Attard et al. (2019b). This instrument can capture the entire range of flux-contributing turbulent eddies within the benthic boundary layer, and this information is used to approximate the benthic O_2 flux non-invasively (Berg et al., 2003; Berg et al., 2022). The instrument recorded co-located measurements of the vertical velocity (w) and the O_2 concentration (C) at 32 Hz, and the data were processed using a multiple-step protocol detailed in Attard et al. (2019b) to extract and quality-check benthic fluxes. The data streams for w and C were decomposed into mean and fluctuating components using Reynolds decomposition, as $w = \bar{w} + w'$ and $C = \bar{C} + C'$ (Berg et al., 2003). The turbulent flux (J_{EC}) was then computed in units of mmol O_2 m^{-2} h^{-1} as $J_{EC} = \overline{w'C'}$, where the overbar represents a period of 15 min. The turbulent flux was then summed with a storage correction term to calculate the total benthic flux ($J_{benthic}$, mmol O_2 m^{-2} h^{-1}) (Rheuban et al., 2014), as:

$$J_{benthic} = J_{EC} + \int_0^h \frac{\partial C}{\partial t} \mathrm{d}z$$

The storage correction term was defined as an average of the O_2 sensors located within and above the canopy (Camillini et al., 2021). The high-frequency time series were also analyzed to identify any pulses of low O_2 waters originating from within the canopy and propagating up into the water column.

2.4. Benthic metabolic rates

The O_2 flux time series was separated into individual 24 h periods (midnight to midnight). The daytime flux ($Flux_{day}$, mmol O_2 m^{-2} h^{-1}) was computed as a bulk average of fluxes measured when PAR > 1.0 µmol m^{-2} s^{-1}. The nighttime flux ($Flux_{night}$, mmol O_2 m^{-2} h^{-1}) was calculated as the average of the remaining fluxes, when PAR < 1.0 µmol m^{-2} s^{-1}. These two values and the number of daylight hours (h_{day}) were used to estimate the daily photosynthetic rate, termed the gross primary

https://doi.org/10.5194/bg-2022-119
Preprint. Discussion started: 19 May 2022

production (*GPP*, in mmol O_2 m^{-2} d^{-1}), as $GPP = Flux_{day} + abs(Flux_{night}) * h_{day}$, and daily respiration (*R*, in mmol O_2 m^{-2} d^{-1}), as $R = abs(Flux_{night}) * 24$, assuming a light-independent respiration rate. The daily balance between *GPP* and *R*, termed the net ecosystem metabolism (*NEM*, in mmol O_2 m^{-2} d^{-1}) was estimated as $NEM = GPP - R$ (Attard et al., 2019b).

The relationship between seafloor PAR and the in situ benthic O_2 flux was investigated using light-saturation curves. Hourly O_2 fluxes were plotted against the corresponding near-bed incident PAR and the relationship between the two was investigated using a modified tangential hyperbolic function by Platt et al. (1980), as $O_2\ flux = P_m * \tanh\left(\frac{\alpha I}{P_m}\right) - R$, where P_m is the maximum rate of hourly gross primary production, α is the initial quasi-linear increase in O_2 flux with PAR, *I* is near-bed irradiance (PAR), and *R* is the dark respiration rate. The photosaturation parameter, I_k (µmol PAR m^{-2} s^{-1}) was derived as P_m/α. Non-linear curve fitting was performed in OriginPro 2020 using a Levenberg–Marquardt iteration algorithm, until a Chi-Squared tolerance value of 1E-9 was reached (Attard and Glud, 2020).

2.5. Biodiversity sampling

At all six sites, we aimed to obtain a quantitative understanding of the abundance, biomass, and species richness of macrophytes and macrofauna (infauna and epifauna). The different habitats required different sampling strategies, since four sites were sedimentary (bare sediments site, two seagrass sites, and the detritus sites) and two sites were rocky (two macroalgal sites) (Rodil et al., 2019).

At the time of our study, the detritus site had a ~20-cm thick detritus mat covering the seabed sediments. The detritus canopy was sampled using large stainless steel core liners (inner diameter = 19 cm; *n* = 4) capable of cutting through the mat, and the collected samples were transferred into a fine-mesh bag. In the laboratory, the detritus was rinsed through a 0.5 mm sieve to collect the associated epifauna. Samples of algal detritus were dried at 60°C for 48 hours and the biomass was calculated as dry weight /m^2.

Macroinfauna at the four sedimentary habitats was sampled using six sediment cores (inner diameter = 5.0 cm, depth = 15 cm). The samples were sieved through a 0.5 mm sieve and animals were stored in alcohol for later identification. At the seagrass sites, representative macrophyte samples were collected by divers from an area around the tripod frame at the end of the deployment using four randomly-placed quadrats (20 x 20 cm). The seagrass within each quadrat was gently

https://doi.org/10.5194/bg-2022-119
Preprint. Discussion started: 19 May 2022

192 uprooted and was transferred into a net-bag. In the laboratory, the samples were rinsed through a
193 0.5 mm sieve to collect all the associated epifauna. The animals were stored in alcohol for later
194 identification, and the seagrass was frozen in sealed bags for further processing. The seagrass
195 samples were later thawed, and the length (cm) of each shoot was measured to determine the
196 average length of the canopy. Individual shoots were counted to determine the canopy density in
197 m^2. The above- and below-ground macrophyte biomass was separated, dried at 60°C for 48 hours
198 and weighed.

199 At the rocky sites, *F. vesiculosus* individuals (n = 4) were randomly collected from around the
200 instrument in fine-mesh bags. Randomly-placed quadrats (1 m^2, n = 4) were used to quantify the
201 number of *F. vesiculosus* individuals per m^2. At the laboratory, the collected *F. vesiculosus* samples
202 were carefully rinsed through a 0.5 mm sieve to collect the epifauna. The height of the *F.*
203 *vesiculosus* canopy was determined from the average length of the sampled individuals. Both *F.*
204 *vesiculosus* and epiphytes were separated to the extent possible, dried at 60 °C for 48 h and
205 weighed. To collect any macrofauna on the bare rock beneath the *F. vesiculosus* canopy, Kautsky-
206 type samplers were placed on the seafloor and the 20 cm x 20 cm area was gently scraped using a
207 spoon into a fine-mesh sampling bag. In the laboratory, all the macrofauna from the four replicates
208 were sieved through a 0.5 mm sieve and stored in alcohol.

209 The fauna from all habitats was sorted, identified to species level, counted, and weighed. The wet
210 weight for each species was noted with 0.0001 g accuracy. In cases where the fauna occurred in
211 very high numbers, the sample was placed in a water-filled tray and divided into eight sectors. Four
212 sectors were randomly chosen to calculate abundance and biomass. The length of gastropods and
213 bivalves was measured from anterior to posterior axis using Vernier callipers (accuracy = 0.01 mm)
214 for conversion to ash-free dry mass (AFDM). The AFDM of bivalves and gastropods was
215 calculated using established relationships between length and weight for Baltic Sea fauna (Rumohr
216 et al., 1987).
217 The abundance (ind m^{-2}) and biomass (AFDM/SFDM g m^{-2}) of the invertebrates across sites were
218 calculated. Primer (v.7 and PERMANOVA+) software was used to perform the nonmetric
219 multidimensional scaling (nMDS, with fourth-root-transformed data) to visualize macrofauna
220 assemblages between sites. ANOSIM based on the Bray-Curtis similarity matrix was also
221 performed in Primer (site as a fixed factor, 4999 random sample permutations) to compare
222 differences in macrofauna abundance and biomass between sites.
223

https://doi.org/10.5194/bg-2022-119
Preprint. Discussion started: 19 May 2022


Biogeosciences Discussions Open Access EGU

3. Results

3.1. Environmental conditions

Average water depth ranged from 2.0 m to 4.0 m at the six study sites, and average water temperature ranged from 9 °C to 16 °C during the study period (Table 1). Hypoxic conditions were only detected at the detritus site. Bottom-water [O_2] at the detritus site ranged from 1 µmol L^{-1} to 429 µmol L^{-1}, with hypoxic conditions occurring for 27 h out of the 120 h long deployment (i.e. for 23 % of the time) (Table 1). At the five other measurement sites, [O_2] were well above hypoxic conditions, with overall concentrations following diel patterns and ranging from 250 µmol L^{-1} to 490 µmol L^{-1} (Table 1).

3.2. Oxygen dynamics in detritus canopies

The oxygen measurements within the detrital canopy document a highly dynamic O_2 environment driven by light availability and flow velocity (Fig. 2). Within the upper layers of the canopy (i.e. ~10 to 25 cm above the seafloor), [O_2] and temporal dynamics largely follow diel patterns driven by light availability, with large ~250 µmol L^{-1} diel excursions in O_2. In the upper canopy region, the [O_2] was lowest in the morning (~160 µmol L^{-1}) and highest in the evening (~430 µmol L^{-1}). In all cases, [O_2] within the upper canopy region was above hypoxic thresholds. However, under low average flow velocities < 2 cm s^{-1}, [O_2] within the lower canopy region (< 10 cm) deviated substantially from the conditions above. No diel variations in O_2 were observed during these periods, and [O_2] rapidly became hypoxic for sustained periods (> 24 h long), with [O_2] being very low (< 10 µmol L^{-1}) during ~10 hr (~8 % of the time) (Fig. 2). As hypoxia persisted throughout the night under low flow velocities, low [O_2] extended upwards into the canopy. Hypoxic conditions ended at the onset of higher mean flow velocities of ~7 cm s^{-1}, which initiated a rapid (i.e. within 1.5 hr) oxygenation of the entire canopy.

https://doi.org/10.5194/bg-2022-119
Preprint. Discussion started: 19 May 2022

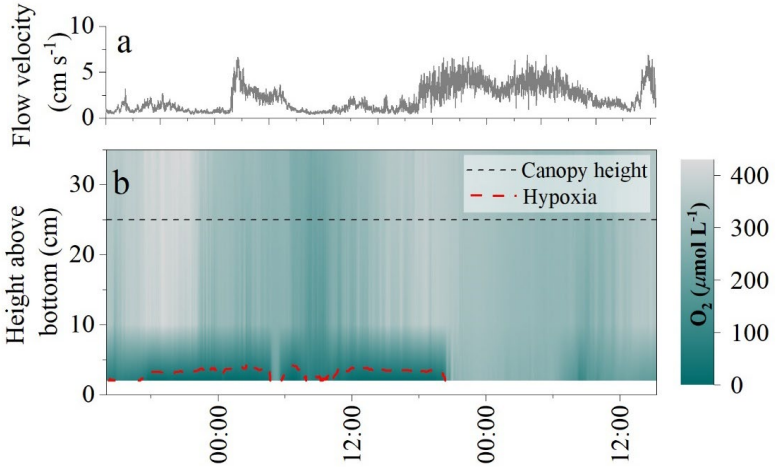

Fig. 2: (a) Flow velocity measured by the velocimeter 10 cm above the detritus canopy and (b) O_2 distribution within the canopy as resolved by three O_2 sensors located at 3 cm, 10 cm, and 35 cm above the seafloor.

3.3. Pulses of hypoxic waters

High-frequency O_2 measurements performed 10 cm above the detritus canopy document transient pulses of hypoxic water originating from within the canopy and propagating upwards into the water column (Fig 3). Such pulses typically followed quiescent weather and occurred at the onset of increased flow velocities. It took < 1 min to reduce [O_2] in the water column from 220 µmol L^{-1} to 65 µmol L^{-1}. Subsequently, a recovery period followed where O_2 gradually increased back to previous concentrations over a ~5 min period. These rapid variations in water column [O_2] were not captured by the slow-response O_2 optode sampling at 1 min intervals.

https://doi.org/10.5194/bg-2022-119
Preprint. Discussion started: 19 May 2022

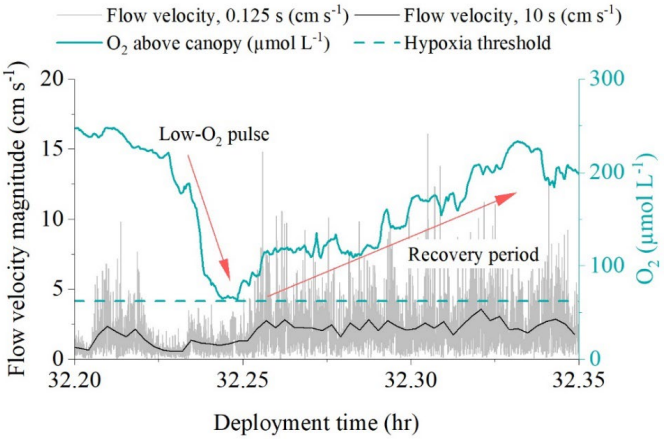

Figure 3: High-frequency [O_2] measured 10 cm above the detrital canopy documents pulses of hypoxic water originating from within the canopy and propagating upwards into the water column.

3.4. Benthic O_2 fluxes and detritus metabolic rates

The eddy covariance measurements at the detritus site produced three days of continuous flux data in June 2017, three days of data in September 2017, and five days of data in June 2018. Benthic O_2 fluxes documented a dynamic O_2 exchange rate driven by light availability and flow velocity (Fig. 4). During quiescent periods with low flow velocity < 2 cm s^{-1}, a clear diel signal in the O_2 flux was observed, indicating substantial primary production associated to the detritus canopy. Higher flow velocities stimulated O_2 uptake rates by up to 5-fold, indicating that canopy ventilation through mixing increased O_2 uptake (Fig. 4).

https://doi.org/10.5194/bg-2022-119
Preprint. Discussion started: 19 May 2022

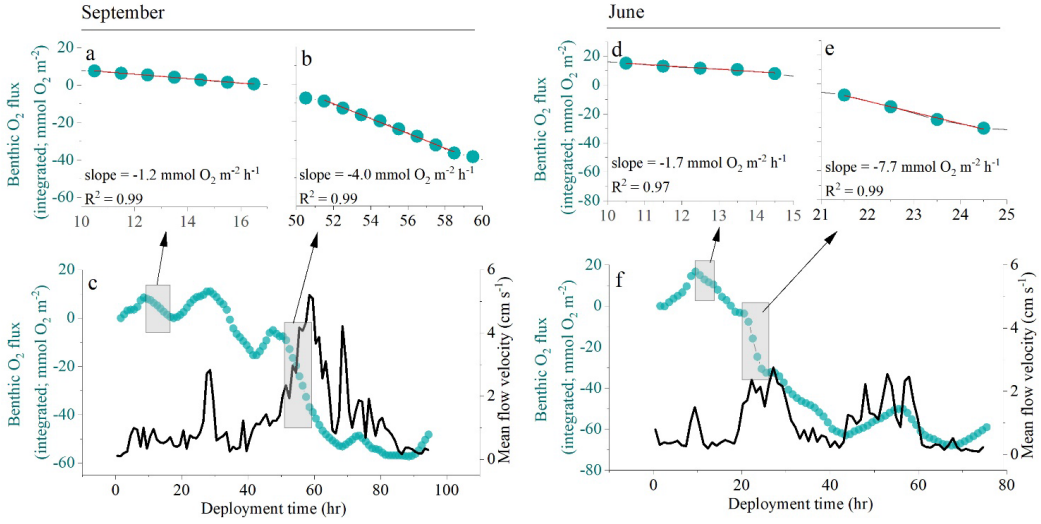

Fig 4: Eddy covariance O_2 fluxes measured 10 cm above the canopy in September (a-c) and June (d-f). Oxygen consumption rates during quiescent periods (panels a and d) were 3.3- and 4.5-fold lower than fluxes measured during more turbulent periods (panels b and e), indicating that canopy ventilation through mixing stimulated O_2 uptake.

Hourly O_2 fluxes ranged from -22 mmol O_2 m^{-2} h^{-1} at night to 13 mmol O_2 m^{-2} h^{-1} during the day and showed a distinct diel cycle in response to sunlight availability (Fig. 5). Daily R ranged from 26 to 97 mmol O_2 m^{-2} d^{-1}, and daily GPP was between 15 and 74 mmol O_2 m^{-2} d^{-1}. Daily R exceeded GPP in all 11 measurement days (net heterotrophic), with NEM ranging from -7 to -32 mmol O_2 m^{-2} d^{-1} (Fig. 5). The deployment average (± SD) GPP:R for the detritus canopy was 0.77 ± 0.04 in June 2017 (n = 3), 0.55 ± 0.02 in September 2017 (n = 3), and 0.77 ± 0.00 in June 2018 (n = 5), and the global mean was 0.71 ± 0.11 (n = 11).

https://doi.org/10.5194/bg-2022-119
Preprint. Discussion started: 19 May 2022

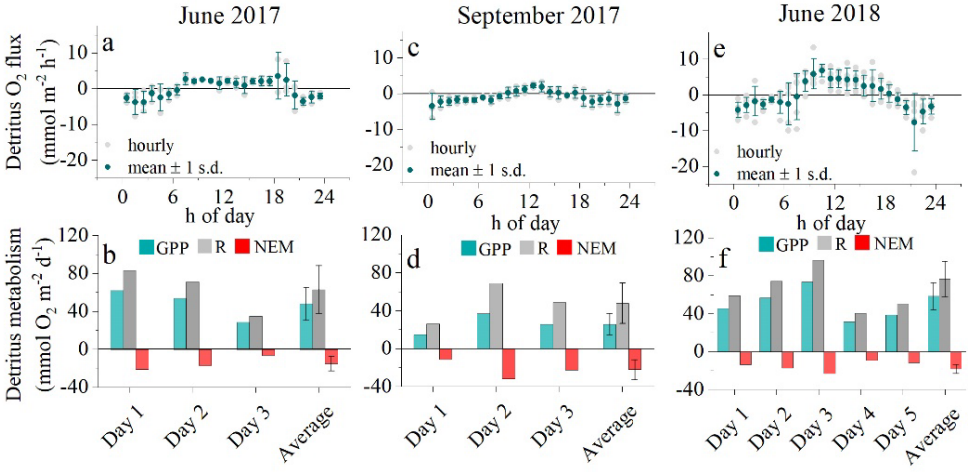

283

284 Fig. 5: Hourly O_2 fluxes (a, c, e) and daily metabolism estimates of gross primary production
285 (GPP), respiration (R), and net ecosystem metabolism (NEM) for the detritus canopy (b, d, f)

286 There was a significant positive relationship between near-bed incident PAR and the benthic O_2
287 flux (Fig. 6). Light-saturation curves fitted to hourly data from all deployments indicated a
288 maximum gross primary production rate (P_m) of 5.14 ± 0.56 mmol O_2 m^{-2} h^{-1}, an α of 0.03 ± 0.01,
289 and a R rate of 1.92 ± 0.26 mmol O_2 m^{-2} h^{-1}. Light saturation (I_k) of the detritus canopy occurred at
290 irradiances greater than ~170 µmol PAR m^{-2} s^{-1}.

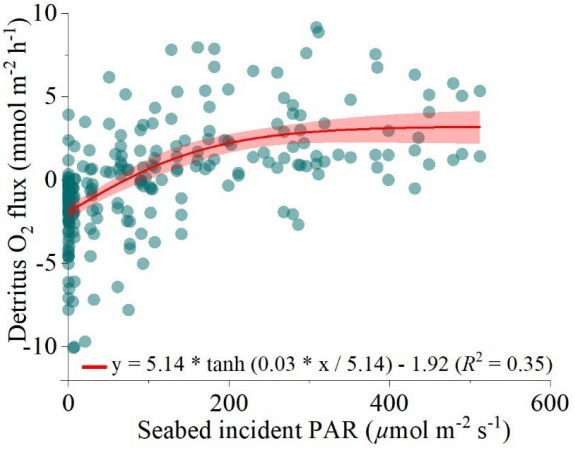

291

https://doi.org/10.5194/bg-2022-119
Preprint. Discussion started: 19 May 2022

292 Fig. 6: Relationship between all hourly in situ benthic O_2 fluxes at the detritus site and light
293 availability from the three flux datasets measured. A modified photosynthesis-irradiance curve by
294 Platt et al. (1980) is shown together with 95% confidence bands.

295 *3.5. Macrobenthic diversity and abundance*

296 The detritus site had a biomass of accumulated macrophyte (*F. vesiculosus*) detritus of 1666 ± 223
297 g dry weight m^{-2} (mean ± SE, $n = 4$), approximately 1.5-fold larger than nearby intact *F. vesiculosus*
298 canopies (Table 2). Detritus accumulation in the five other habitats was around 100-fold smaller.
299 The area of the detritus site estimated using Google Earth was 2300 m^2, amounting to 3,832 kg dry
300 weight of *F. vesiculosus* fragments. Macrofauna abundance ranged from 2719 ± 854 ind. m^{-2} at the
301 bare sediments site to 17259 ± 2421 ind. m^{-2} at the sheltered *F. vesiculosus* site (mean ± SE, $n = 4$)
302 (Table 3). Macrofauna biomass ranged from 6 ± 2 g m^{-2} at the bare site to 41 ± 9 g m^{-2} at the
303 exposed seagrass site (mean ± SE, $n = 4$), and the number of species ranged from 6 to 23, with the
304 lowest values measured at the bare sediments and detritus sites, and the highest values at the
305 sheltered *F. vesiculosus* site (Table 3).

306 At the detritus site, there was a low abundance of epifaunal crustaceans when compared to other
307 habitats with canopies. Key species, such as the amphipod *Gammarus spp.* were notably absent, and
308 isopods such as *Idotea spp.* were present in low abundance (Table A1). Similarly, there was a
309 notable absence of bivalves such as the soft-shelled clam, *Mya arenaria*, and the cockle
310 *Cerastoderma glaucum*. Polychaetes such as *Hediste diversicolor* and *Marenzelleria spp*. were also
311 absent from the detritus site but present in other sedimentary habitats (Table A1). The nMDS
312 ordination of the macrofaunal assemblages indicated a clear separation of points representing the
313 different habitat sites (ANOSIM: $R^2 = 0.865$; $p < 0.001$). The assemblages from the bare sand and
314 the detritus sites formed separated site groupings compared to the vegetated sites ('*Fucus*' and
315 'seagrass', both exposed and sheltered). Within the vegetated sites, the assemblages of the 'seagrass
316 sheltered' and the '*Fucus* sheltered' sites were the most different (Fig. 7).

317

https://doi.org/10.5194/bg-2022-119
Preprint. Discussion started: 19 May 2022

318 Table 2: Vegetation abundance and biomass (dry weight) at the six study sites. Abundance is shoots
319 per m^2 for seagrass and individuals per m^2 for *F. vesiculosus*. Values are mean ± SE.

Site	Abundance per m^2	Above-ground biomass (g m^{-2})	Belowground biomass (g m^{-2})	Detritus (g m^{-2})	Biomass other species (g m^{-2})
Macrophyte detritus	-	-	-	1666 ± 223	-
Bare sediments	-	-	-	-	-
Sheltered *Z. marina*	768 ± 92	21 ± 2	8 ± 1	58 ± 13	0.1 ± 0.1
Exposed *Z. marina*	2565 ± 164	69 ± 7	25 ± 3	16 ± 2	0.2 ± 0.2
Sheltered *F. vesiculosus*	16 ± 2	1244 ± 58	-	55 ± 11	-
Exposed *F. vesiculosus*	16 ± 2	1112 ± 119	-	20 ± 2	-

320

321 Table 3: Macrofauna abundance, biomass (ash-free dry weight), and number of species at the six
322 study sites.

Site	Infauna abundance (ind. m^{-2})	Epifauna abundance (ind. m^{-2})	Total abundance (ind. m^{-2})	Infauna biomass (g m^{-2})	Epifauna biomass (g m^{-2})	Total biomass (g m^{-2})	Number of species
Macrophyte detritus	4175 ± 2885	493 ± 37	4668 ± 2885	5 ± 3	5 ± 0	9 ± 3	6
Bare sediments	2719 ± 854	-	2719 ± 854	6 ± 2	-	6 ± 2	6
Sheltered *Z. marina*	6110 ± 787	3020 ± 874	9130 ± 1176	30 ± 6	2 ± 0	33 ± 6	18
Exposed *Z. marina*	6959 ± 620	3316 ± 772	10275 ± 990	31 ± 8	10 ± 2	41 ± 9	16
Sheltered *F. vesiculosus*	-	17259 ± 2421	17259 ± 2421	-	11 ± 2	11 ± 2	23
Exposed *F. vesiculosus*	-	3551 ± 609	3551 ± 609	-	7 ± 2	7 ± 2	12

323

https://doi.org/10.5194/bg-2022-119
Preprint. Discussion started: 19 May 2022

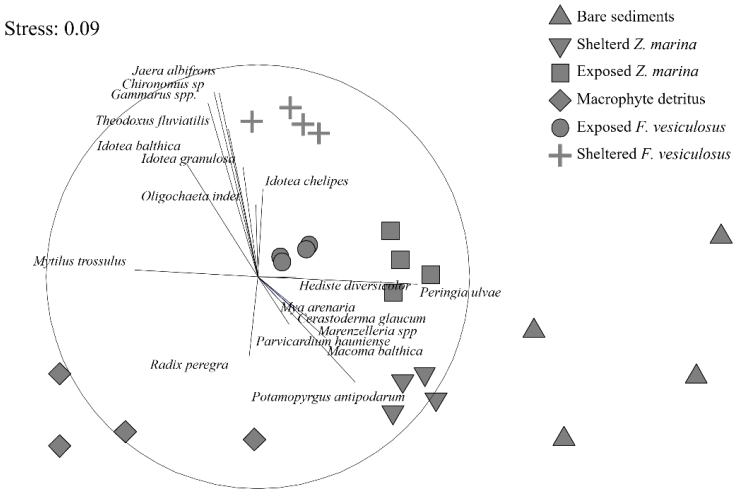

Fig. 7: A non-metric multidimensional scaling (nMDS) ordination of the macrofaunal assemblages indicated a clear separation of points representing the different habitat sites. The assemblages from the bare sand and the detritus sites formed separate site groupings compared to the vegetated sites.

4. Discussion

4.1. Detritus metabolism rates

The eddy covariance measurements document a highly active detrital canopy that photosynthesized as well as respired. High daily rates of GPP of up to 75 mmol O_2 m^{-2} d^{-1} and R of 100 mmol O_2 m^{-2} d^{-1} are comparable to some of the most productive habitats in the area, such as dense seagrass meadows (*Zostera marina*) and intact canopies of bladder wrack (*Fucus vesiculosus*) (Attard et al., 2019b). These results indicate that shallow detritus accumulation zones are not just regions of organic matter remineralization, but rather they synthesize substantial amounts of organic matter through primary production. The range in daily GPP:R from 0.53 to 0.81 indicates that primary production can offset a substantial proportion of the respiratory demand, which extends the persistence of detritus in the coastal zone. These observations are consistent with the laboratory study by Frontier et al. (2021), who determined that following detachment, kelp (*Laminaria hyperborea* and *L. ochroleuca*) fragments retain physiological and reproductive capabilities for up to several months. Carbon retention within the coastal zone and export to deeper, sedimentary accumulation regions would therefore be larger than would be predicted by decomposition theory alone. Similarly, slow, and incomplete degradation of algae detritus under low O_2 conditions, which could occur, for instance, in the bottom layers of detrital canopies or in the large anoxic basins of

https://doi.org/10.5194/bg-2022-119
Preprint. Discussion started: 19 May 2022

345 the Baltic Sea (Conley et al., 2009), would increase carbon retention, transfer, and sequestration
346 potential (Pedersen et al., 2021).

347 *4.2. 'Hidden' benthic hypoxia*

348 Our in situ measurements performed over a few days in late spring document that subtidal detritus
349 accumulation zones uniquely experience dynamic O_2 conditions driven by sunlight availability and
350 flow velocity, with rapid O_2 oscillations and frequent periods of hypoxia (Table 1). Hypoxic
351 conditions were largely restricted to the lower ~5 cm of the canopy and were only revealed by
352 sensors placed directly above the sediment surface (< 5 cm distance). At the onset of wave-driven
353 mixing, hypoxic waters from within the canopy propagated upwards into the water column and
354 were registered by fast-response O_2 sensors located 10 cm above the canopy (~35 cm above the
355 seafloor). This observation suggests that the O_2 conditions inside the entire canopy and even in the
356 water column directly above can reach hypoxic conditions for a few minutes (Fig. 4). Such pulses,
357 however, were not registered by the slow-response O_2 optodes with a factory-specified $T_{90} < 2$ min.
358 The minimum O_2 concentration observed by these sensors placed at 10 cm and 35 cm above the
359 seafloor was 158 and 229 µmol L^{-1}, respectively, and thus well above hypoxic conditions.

360 The importance of measuring O_2 close to the seafloor was demonstrated more than 40 years ago by
361 Jorgensen (1980), who developed a small sled that could be towed slowly across the seafloor to
362 map spatial gradients in O_2 at < 5 cm distance to the seabed. Since then, other researchers have
363 investigated the distribution of dissolved constituents such as O_2 and nutrients in the benthic
364 boundary layer using motor-driven sliders that transport sensors vertically towards the seafloor
365 (Holtappels et al., 2011). These studies document that solute gradients are largest near the seafloor,
366 because the seafloor is a strong solute sink or source, and turbulent diffusivities are low. For
367 practical reasons, however, coastal monitoring programs measure O_2 further away from the
368 seafloor. It is therefore likely that hypoxia in the coastal zone is currently underestimated because
369 large-scale models are based on measurements performed higher above the seafloor (0.5-1.0 m)
370 (Virtanen et al., 2019).

371 *4.3. Biodiversity and oxygen dynamics in detritus canopies*

372 Despite being considered a temporary habitat, detritus was found in abundance at our study site on
373 all occasions in May, June, and September. This type of habitat is likely quite widespread in the
374 Baltic. Topographical depressions with limited water exchange occupy ~1350 km^2 or ~11% of the

https://doi.org/10.5194/bg-2022-119
Preprint. Discussion started: 19 May 2022

northern Baltic Sea (Virtanen et al., 2019). During a recent seasonal study, we observed the highest abundance of detritus at our study site in summer and autumn, coinciding with high southerly winds that erode intact canopies in shallower waters (Attard et al., 2019a). However, we also observed significant canopy erosion in winter when a substantial biomass of *F. vesiculosus* froze into sea ice and got dislodged once the ice broke up (Fig. 8). Therefore, some degree of drifting detritus might be common throughout the year. Drifting detritus constitutes a significant habitat structure. Given high enough biomass, however, detritus canopies can be a challenging habitat for most species. Dense canopies induce drag, suppress local turbulence, and curb the exchange of O_2 and other nutrients between the benthic boundary layer and the seafloor (Hansen and Reidenbach, 2017). If O_2 consumption within the canopy and underlying sediments exceeds O_2 supply from the water column, low-O_2 conditions develop, resulting in hotspots of anoxia and hydrogen sulfide production, inducing mortality of sedentary species (Norkko and Bonsdorff, 1996a; Glud et al., 2004; Norkko et al., 2013). At our study site, hypoxic conditions uniquely occurred at the detritus site and for around a quarter of the deployment time (Table 1). We can expect these conditions to be particularly challenging for crustaceans, the most hypoxia-sensitive macroinvertebrate group (Vaquer-Sunyer and Duarte, 2008). Indeed, we only found one crustacean species at this site- the isopod *Idotea balthica* (Table A1)- which is mobile and can tolerate hypoxic conditions for a few hours (Vetter and Dayton, 1999). All other invertebrates observed at the detritus site were mollusks (Table A1), the most hypoxia-tolerant marine invertebrate group (Vaquer-Sunyer and Duarte, 2008). Other tolerant species include the blue mussel *Mytilus trossulus x edulis* that can survive > 300 h of anoxia (Jorgensen, 1980), although the survival of larvae depends on its developmental stage (Diaz and Rosenberg, 1995). Similarly, the mudsnail *Peringia ulvae* is highly mobile and can survive > 150 h of anoxia (Jorgensen, 1980; Norkko et al., 2000).

Overall, the dynamic O_2 conditions in detrital canopies seem to be challenging for most species in this region of the Baltic Sea, with lethal and non-lethal thresholds frequently being exceeded on timescales of hours to days. We currently have a poor understanding of the extent of 'hidden' hypoxia in coastal waters, because O_2 measurements are performed at some distance away from the seabed. While this is a practical approach that is done to minimize sensor fouling and damage, it does not reveal the full extent of coastal hypoxia. If implemented widely, sensor arrays, as described herein, and sensor elevators (e.g. Holtappels et al. (2011)) can fill in this knowledge gap and provide important insights into the ecological status and biogeochemical cycling that is needed for the sustainable management of coastal ecosystems.

https://doi.org/10.5194/bg-2022-119
Preprint. Discussion started: 19 May 2022

Fig. 8: substantial detritus accumulation was observed in late winter (March 2021) when *F. vesiculosus* froze into sea ice and got dislodged once the ice broke up. (Photo by Alf Norkko)

https://doi.org/10.5194/bg-2022-119
Preprint. Discussion started: 19 May 2022

410 Table A1. Species list for the five studied sites. Presence is indicated by 'x'.

Group	Species	Macrophyte detritus	Bare sediments	Sheltered *Z. marina*	Exposed *Z. marina*	Sheltered *F. vesiculosus*	Exposed *F. vesiculosus*
Crustacea	*Amphibalanus improvisus*			x			
	Asellus aquaticus					x	
	Corophium spp.			x			
	Gammarus spp.			x	x	x	x
	Idotea balthica	x			x	x	x
	Idotea chelipes				x	x	x
	Idotea granulosa			x	x	x	x
	Jaera albifrons			x	x	x	x
	Cladocera					x	
	Copepoda					x	
	Ostracoda sp.					x	
	Mysid					x	x
Bivalvia	*Cerastoderma glaucum*			x	x		
	Parvicardium haunience			x	x		
	Macoma balthica	x	x	x	x	x	x
	Mya arenaria			x	x		
	Mytilus trossulus x edulis	x		x	x	x	x
Gastropoda	*Peringia ulvae*	x	x	x	x	x	x
	Radix sp.	x		x			x
	Potamopyrgus antipodarum		x	x			
	Theodoxus fluviatilis	x	x	x	x	x	x

https://doi.org/10.5194/bg-2022-119
Preprint. Discussion started: 19 May 2022

Polychaeta	*Hediste diversicolor*			x	x		
	Halicryptus spinulosus					x	
	Maranzelleria spp.		x	x	x	x	
	Nematoda					x	
	Oligochaeta			x	x	x	
	Pygospio elegans					x	
Others	*Chironomus* sp			x	x	x	x
	Coleoptera larvae						x
	Odonata						x
	Cyanophthalma obscura						x
	Hydrachnidae		x				x

411

https://doi.org/10.5194/bg-2022-119
Preprint. Discussion started: 19 May 2022

Author contribution

All authors contributed significantly to designing the research, funding the study, collecting the data, analyzing samples and data, and interpreting the results. KMA wrote the paper with input from all authors.

Competing interests

The authors declare that they have no conflict of interest

Data availability

All data presented in this paper will be made available in a FAIR-aligned data repository upon acceptance of the paper.

Acknowledgements

Colleagues at the Tvärminne Zoological Station provided help with fieldwork and logistics. Anni Glud at the University of Southern Denmark constructed the oxygen microsensors used in this study. Elina Virtanen at the Finnish Environmental Institute (SYKE) provided spatial data used to estimate the potential extent of detritus canopies. The Walter and Andrée de Nottbeck Foundation supported this work through a postdoctoral fellowship to KMA and through a Masters fellowship to AL. Further funding for this project was provided by research grants from the Academy of Finland (project ID 294853), the University of Helsinki and Stockholm University strategic fund for collaborative research (the Baltic Bridge initiative), and Denmark's Independent Research Fund (project ID 7014-00078). This study has utilized research infrastructure facilities provided by FINMARI (Finnish Marine Research Infrastructure network, The Academy of Finland, project ID 283417).

https://doi.org/10.5194/bg-2022-119
Preprint. Discussion started: 19 May 2022

References

Attard, K. M. and Glud, R. N.: Technical Note: Estimating light-use efficiency of benthic habitats using underwater O-2 eddy covariance, Biogeosciences, 17, 4343-4353, 2020.

Attard, K. M., Rodil, I. F., Berg, P., Norkko, J., Norkko, A., and Glud, R. N.: Seasonal metabolism and carbon export potential of a key coastal habitat: The perennial canopy-forming macroalga *Fucus vesiculosus*, Limnol Oceanogr, 64, 149-164, 10.1002/lno.11026, 2019a.

Attard, K. M., Rodil, I. F., Glud, R. N., Berg, P., Norkko, J., and Norkko, A.: Seasonal ecosystem metabolism across shallow benthic habitats measured by aquatic eddy covariance, Limnology and Oceanography Letters, 4, 79-86, 10.1002/lol2.10107, 2019b.

Berg, P. and Pace, M. L.: Continuous measurement of air-water gas exchange by underwater eddy covariance, Biogeosciences, 14, 5595-5606, 2017.

Berg, P., Huettel, M., Glud, R. N., Reimers, C. E., and Attard, K. M.: Aquatic Eddy Covariance: The Method and Its Contributions to Defining Oxygen and Carbon Fluxes in Marine Environments, Annual Review of Marine Science, 14, 431-455, 10.1146/annurev-marine-042121-012329, 2022.

Berg, P., Røy, H., Janssen, F., Meyer, V., Jorgensen, B. B., Huettel, M., and de Beer, D.: Oxygen uptake by aquatic sediments measured with a novel non-invasive eddy-correlation technique, Marine Ecology Progress Series, 261, 75-83, 10.3354/Meps261075, 2003.

Bittig, H. C., Kortzinger, A., Neill, C., van Ooijen, E., Plant, J. N., Hahn, J., Johnson, K. S., Yang, B., and Emerson, S. R.: Oxygen Optode Sensors: Principle, Characterization, Calibration, and Application in the Ocean, Frontiers in Marine Science, 4, 2018.

Breitburg, D., Levin, L. A., Oschlies, A., Gregoire, M., Chavez, F. P., Conley, D. J., Garcon, V., Gilbert, D., Gutierrez, D., Isensee, K., Jacinto, G. S., Limburg, K. E., Montes, I., Naqvi, S. W. A., Pitcher, G. C., Rabalais, N. N., Roman, M. R., Rose, K. A., Seibel, B. A., Telszewski, M., Yasuhara, M., and Zhang, J.: Declining oxygen in the global ocean and coastal waters, Science, 359, 46-+, 2018.

Broch, O. J., Hancke, K., and Ellingsen, I. H.: Dispersal and Deposition of Detritus From Kelp Cultivation, Frontiers in Marine Science, 9, 2022.

Broch, O. J., Alver, M. O., Bekkby, T., Gundersen, H., Forbord, S., Handa, A., Skjermo, J., and Hancke, K.: The Kelp Cultivation Potential in Coastal and Offshore Regions of Norway, Frontiers in Marine Science, 5, 2019.

Camillini, N., Attard, K. M., Eyre, B. D., and Glud, R. N.: Resolving community metabolism of eelgrass Zostera marina meadows by benthic flume-chambers and eddy covariance in dynamic coastal environments, Marine Ecology Progress Series, 661, 97-114, 2021.

Conley, D. J., Bjorck, S., Bonsdorff, E., Carstensen, J., Destouni, G., Gustafsson, B. G., Hietanen, S., Kortekaas, M., Kuosa, H., Meier, H. E. M., Muller-Karulis, B., Nordberg, K., Norkko, A., Nurnberg, G., Pitkanen, H., Rabalais, N. N., Rosenberg, R., Savchuk, O. P., Slomp, C. P., Voss, M., Wulff, F., and Zillen, L.: Hypoxia-Related Processes in the Baltic Sea, Environ Sci Technol, 43, 3412-3420, 10.1021/es802762a, 2009.

Davanzo, C. and Kremer, J. N.: Diel Oxygen Dynamics and Anoxic Events in an Eutrophic Estuary of Waquoit Bay, Massachusetts, Estuaries, 17, 131-139, 1994.

Diaz, R. J. and Rosenberg, R.: Marine benthic hypoxia: A review of its ecological effects and the behavioural responses of benthic macrofauna, Oceanography and Marine Biology - an Annual Review, Vol 33, 33, 245-303, 1995.

Diaz, R. J. and Rosenberg, R.: Spreading dead zones and consequences for marine ecosystems, Science, 321, 926-929, 10.1126/science.1156401, 2008.

Duarte, C. M. and Cebrián, J.: The fate of marine autotrophic production, Limnol Oceanogr, 41, 1758-1766, DOI 10.4319/lo.1996.41.8.1758, 1996.

https://doi.org/10.5194/bg-2022-119
Preprint. Discussion started: 19 May 2022

480 Frontier, N., de Bettignies, F., Foggo, A., and Davoult, D.: Sustained productivity and respiration of
481 degrading kelp detritus in the shallow benthos: Detached or broken, but not dead, Mar Environ Res,
482 166, 2021.
483 Garcia, H. E. and Gordon, L. I.: Oxygen Solubility in Seawater - Better Fitting Equations, Limnol
484 Oceanogr, 37, 1307-1312, 1992.
485 Glud, R. N.: Oxygen dynamics of marine sediments, Mar Biol Res, 4, 243-289, 2008.
486 Glud, R. N., Rysgaard, S., Fenchel, T., and Nielsen, P. H.: A conspicuous H2S-oxidizing microbial
487 mat from a high-latitude Arctic fjord (Young Sound, NE Greenland), Mar Biol, 145, 51-60, DOI
488 10.1007/s00227-004-1296-8, 2004.
489 Hansen, J. C. R. and Reidenbach, M. A.: Turbulent mixing and fluid transport within Florida Bay
490 seagrass meadows, Adv Water Resour, 108, 205-215, 2017.
491 Holtappels, M., Kuypers, M. M. M., Schluter, M., and Bruchert, V.: Measurement and
492 interpretation of solute concentration gradients in the benthic boundary layer, Limnol Oceanogr-
493 Meth, 9, 1-13, 2011.
494 Jorgensen, B. B.: Seasonal Oxygen Depletion in the Bottom Waters of a Danish Fjord and Its Effect
495 on the Benthic Community, Oikos, 34, 68-76, 1980.
496 Krumhansl, K. A. and Scheibling, R. E.: Production and fate of kelp detritus, Marine Ecology
497 Progress Series, 467, 281-302, 10.3354/meps09940, 2012.
498 Long, M. H. and Nicholson, D. P.: Surface gas exchange determined from an aquatic eddy
499 covariance floating platform, Limnol Oceanogr-Meth, 16, 145-159, 2018.
500 McGinnis, D. F., Cherednichenko, S., Sommer, S., Berg, P., Rovelli, L., Schwarz, R., Glud, R. N.,
501 and Linke, P.: Simple, robust eddy correlation amplifier for aquatic dissolved oxygen and hydrogen
502 sulfide flux measurements, Limnol Oceanogr-Meth, 9, 340-347, DOI 10.4319/lom.2011.9.340,
503 2011.
504 Middelburg, J. J. and Levin, L. A.: Coastal hypoxia and sediment biogeochemistry, Biogeosciences,
505 6, 1273-1293, DOI 10.5194/bg-6-1273-2009, 2009.
506 Norkko, A. and Bonsdorff, E.: Population responses of coastal zoobenthos to stress induced by
507 drifting algal mats, Marine Ecology Progress Series, 140, 141-151, DOI 10.3354/meps140141,
508 1996a.
509 Norkko, A. and Bonsdorff, E.: Rapid zoobenthic community responses to accumulations of drifting
510 algae, Marine Ecology Progress Series, 131, 143-157, DOI 10.3354/meps131143, 1996b.
511 Norkko, A., Villnas, A., Norkko, J., Valanko, S., and Pilditch, C.: Size matters: implications of the
512 loss of large individuals for ecosystem function, Sci Rep-Uk, 3, ARTN 2646

513 10.1038/srep02646, 2013.
514 Norkko, J., Bonsdorff, E., and Norkko, A.: Drifting algal mats as an alternative habitat for benthic
515 invertebrates: Species specific responses to a transient resource, Journal of Experimental Marine
516 Biology and Ecology, 248, 79-104, 2000.
517 Pedersen, M. F., Filbee-Dexter, K., Frisk, N. L., Sarossy, Z., and Wernberg, T.: Carbon
518 sequestration potential increased by incomplete anaerobic decomposition of kelp detritus, Marine
519 Ecology Progress Series, 660, 53-67, 2021.
520 Platt, T., Gallegos, C. L., and Harrison, W. G.: Photoinhibition of photosynthesis in natural
521 assemblages of marine phytoplankton, J Mar Res, 38, 687-701, 1980.
522 Rheuban, J. E., Berg, P., and McGlathery, K. J.: Multiple timescale processes drive ecosystem
523 metabolism in eelgrass (*Zostera marina*) meadows, Marine Ecology Progress Series, 507, 1-13,
524 10.3354/meps10843, 2014.
525 Robertson, E. K., Roberts, K. L., Burdorf, L. D. W., Cook, P., and Thamdrup, B.: Dissimilatory
526 nitrate reduction to ammonium coupled to Fe(II) oxidation in sediments of a periodically hypoxic
527 estuary, Limnol Oceanogr, 61, 365-381, 2016.

https://doi.org/10.5194/bg-2022-119
Preprint. Discussion started: 19 May 2022

528 Rodil, I. F., Attard, K. M., Norkko, J., Glud, R. N., and Norkko, A.: Towards a sampling design for
529 characterizing habitat-specific benthic biodiversity related to oxygen flux dynamics using Aquatic
530 Eddy Covariance, Plos One, 14, e0211673, 10.1371/journal.pone.0211673, 2019.
531 Rumohr, H., Brey, T., and Ankar, S.: A compilation of biometric conversion factors for benthic
532 invertebrates of the Baltic Sea, Baltic Marine Biologists, 9, 1-56, 1987.
533 Smith, S. V.: Marine macrophytes as a global carbon sink, Science, 211, 838-840, DOI
534 10.1126/science.211.4484.838, 1981.
535 Tyler, R. M., Brady, D. C., and Targett, T. E.: Temporal and Spatial Dynamics of Diel-Cycling
536 Hypoxia in Estuarine Tributaries, Estuar Coast, 32, 123-145, 10.1007/s12237-008-9108-x, 2009.
537 Vaquer-Sunyer, R. and Duarte, C. M.: Thresholds of hypoxia for marine biodiversity, P Natl Acad
538 Sci USA, 105, 15452-15457, 10.1073/pnas.0803833105, 2008.
539 Vetter, E. W. and Dayton, P. K.: Organic enrichment by macrophyte detritus, and abundance
540 patterns of megafaunal populations in submarine canyons, Marine Ecology Progress Series, 186,
541 137-148, 1999.
542 Virtanen, E. A., Norkko, A., Sandman, A. N., and Viitasalo, M.: Identifying areas prone to coastal
543 hypoxia - the role of topography, Biogeosciences, 16, 3183-3195, 2019.

544